Cerebellum (2008) 7:547–558
DOI 10.1007/s12311-008-0086-0

Purkinje Cell Input to Cerebellar Nuclei in Tottering: Ultrastructure and Physiology

Freek E. Hoebeek · Sara Khosrovani · Laurens Witter · Chris I. De Zeeuw

Published online: 11 December 2008

Abstract Homozygous tottering mice are spontaneous ataxic mutants, which carry a mutation in the gene encoding the ion pore of the P/Q-type voltage-gated calcium channels. P/Q-type calcium channels are prominently expressed in Purkinje cell terminals, but it is unknown to what extent these inhibitory terminals in tottering mice are affected at the morphological and electrophysiological level. Here, we investigated the distribution and ultrastructure of their Purkinje cell terminals in the cerebellar nuclei as well as the activities of their target neurons. The densities of Purkinje cell terminals and their synapses were not significantly affected in the mutants. However, the Purkinje cell terminals were enlarged and had an increased number of vacuoles, whorled bodies, and mitochondria. These differences started to occur between 3 and 5 weeks of age and persisted throughout adulthood. Stimulation of Purkinje cells in adult tottering mice resulted in inhibition at normal latencies, but the activities of their postsynaptic neurons in the cerebellar nuclei were abnormal in that the frequency and irregularity of their spiking patterns were enhanced. Thus, although the number of their terminals and their synaptic contacts appear quantitatively intact, Purkinje cells in tottering mice show several signs of axonal damage that may contribute to altered postsynaptic activities in the cerebellar nuclei.

Keywords Cerebellum · Degeneration · Calcium channels · Cerebellar nuclei · Ataxia

Introduction

The spontaneous mouse mutant tottering (*tg*) suffers from recessive neurological disorders including both permanent ataxia as well as episodes of dystonia, paroxysmal dyskinesia, and behavioral absence seizures. The absence seizures in *tg* mice resemble human *petit mal* seizures in that they are marked by abnormal electroencephalography (EEG) patterns [1] and that they respond to common antiepileptic drugs [2], whereas the attacks of paroxysmal dyskinesia cannot be correlated reliably to a clear EEG pattern and do not respond to antiepileptic therapeutics [3, 4]. The episodes of paroxysmal dyskinesia can be reliably triggered by environmental challenges [4–6] and are distinguished from the permanent ataxia by the sequence of three stages of behavioral abnormalities, which start at the hind limbs, then gradually spread to the front limbs, and eventually also reach the head and neck. These motor attacks, which typically occur approximately one to two times per day and can last up to 40 min, include irregular jerky movements, slow writhing motions, and involuntary stretching of the muscles [1, 3, 7]. In between these episodes, *tg* mice are mildly ataxic in that they show an abnormal gait and decreased motor performance and learning [8–10].

The genotype of *tg* mice is characterized by an autosomal recessive mutation in the gene located on chromosome 8 that encodes the α_{1A}-subunit of P/Q-type

Freek E. Hoebeek and Sara Khosrovani contributed equally.

F. E. Hoebeek · S. Khosrovani · C. I. De Zeeuw (✉)
Department of Neuroscience, Erasmus MC,
Dr. Molewaterplein 50,
3015 GE Rotterdam, The Netherlands
e-mail: c.dezeeuw@erasmusmc.nl

L. Witter · C. I. De Zeeuw
Netherlands Institute for Neuroscience,
Royal Academy of Arts & Sciences (KNAW),
Meibergdreef 47,
1105 BA Amsterdam, The Netherlands

Ca^{2+}-channels in nerve, muscle, and secretory cells [11, 12]. Since P/Q-type calcium channels are abundantly present in cerebellar Purkinje cells and gate ~90% of their high-voltage-activated Ca^{2+}-influx [13, 14], it is parsimonious to explain the juvenile onset of ataxia in *tg* mutants by deficits in their Purkinje cells. Indeed, the calcium influx in *tg* Purkinje cells is decreased by ~45% [15], their responses to parallel fiber stimulation are reduced by ~50% [16], and their simple spike firing patterns show enhanced irregularities with periods of pauses and bursts [9]. Moreover, Purkinje cells in *tg* show morphological aberrations in that their dendritic spines make relatively frequently multiple contacts with individual parallel fiber varicosities [17] and that their somata have elongated nuclei and are reduced in size [18, 19]. Interestingly, many of the morphological and physiological changes in the Purkinje cell dendrites and somata precede or coincide with the occurrence of the ataxia at the end of the first month of age suggesting that these changes form a major cause of the behavioral deficits [9, 17]. However, it remains possible that changes at the level of the terminals of the Purkinje cells also contribute to the ataxia in *tg* mutants, because the density of P/Q-type Ca^{2+}-channels is particularly high in terminals [20, 21] and because chronically altered firing in Purkinje cells can lead to pathological alterations in their terminals [22]. We therefore investigated the Purkinje cell terminals of *tg* mutants at both the morphological and electrophysiological level. To correlate possible morphological aberrations to the behavioural changes, we investigated the distribution and ultrastructure of Purkinje cell terminals in the cerebellar nuclei before (2–3-week-old animals) and after (5-week and 6-month-old animals) the onset of the ataxia. In addition, we investigated whether the contacts of the Purkinje cell terminals with their postsynaptic neurons in the cerebellar nuclei in the adult mice were functionally intact by recording the extracellular activities of the cerebellar nuclei neurons following stimulation of the Purkinje cells.

Materials and Methods

Animals

Data were collected from 18 *tg* mice and 17 wild-type littermates (both male and female mice were included; C57BL/6J background; originally ordered from Jackson laboratory, Bar Harbor, ME, USA). The presence of the *tg* mutation in the *Cacna1a* gene on chromosome 8 was confirmed by PCR using 3′-TTCTGGGTACCAGA TACAGG-5′ and 5′-AAGTGTCGAAGTTGGTGCGC-3′ primers (Eurogentech, The Netherlands) and subsequent digestion using restriction enzyme *NSBI* at the age of p9–p12. No oligosyndactyly was used. All preparations and experiments were done according to the European Communities Council Directive (86/609/EEC) and were reviewed and approved by the national ethics committee. For light microscopy, we restricted ourselves to animals of 6 months (*tg*, N=3; wild type, N=3), while for electron microscopy, we examined animals at the age of 2–3 weeks (i.e., for both 14 and 20 days *tg*, N=2 and wild type, N=2), 5 weeks (*tg*, N=3; wild type, N=2), and 6 months (*tg*, N=3; wild type, N=3). The electrophysiological recordings were conducted in mice at the age of 6 months (*tg*, N=5; wild type, N=5).

Light Microscopy

In this study, the Purkinje cell terminals were identified by immunocytochemical labeling using anticalbindin labeling [23, 24]. To do so, three adult wild-type and three *tg* littermates were anesthetized with an overdose of Nembutal (i.p.) and transcardially perfused with 0.12 M phosphate buffered saline (pH=7.4) followed by 4% paraformaldehyde in phosphate buffer (PB) at room temperature. The cerebellum and brainstems were carefully removed, post-fixed in 4% paraformaldehyde for 2 h, placed in 10% sucrose in PB at 4°C overnight, and subsequently embedded in gelatin in 30% sucrose. The blocks were cut on a cryotome into coronal sections of 40 μm. Sections were washed in blocking solution containing 10% normal horse serum (NHS) with 0.5% triton for 1 h and incubated in rabbit anticalbindin (1:7,000, Swant) with 2% normal horse serum and 0.5% Triton for 48 h [25]. Subsequently, the sections were incubated for 2 h in biotinylated goat–antirabbit IgG at room temperature (1 to 500; Vector) followed by 2 h in avidin-biotinylated horseradish peroxidase complex (ABC-HRP; Vector). Sections were rinsed in PB and stained with 0.5% 3,3-diaminobenzidine tetrahydrochloride and 0.01% H_2O_2 for 15 min at room temperature. Sections of *tg* mutants and wild-type littermates were processed simultaneously to avoid artificial differences due to the staining procedures. For quantification of terminals in the lateral cerebellar nuclei and interposed nuclei, we framed 500×500 μm with a ten times objective and used Neurolucida systems software (MicroBrightField, Colchester, VT, USA) for analyses, which were done blind to the genotype. The terminal numbers were averaged per animal and nucleus.

Electron Microscopy

Wild-type (N=9) and *tg* mice (N=10) were anesthetized with an overdose of Nembutal (i.p.) and transcardially perfused with 4% paraformaldehyde and 0.5% glutaraldehyde in cacodylate buffer. Brains were removed, kept

overnight in 4% paraformaldehyde, and cut into 80 μm thick coronal sections on a vibratome. The vibratome sections were subsequently washed and blocked for 1 h in 10% NHS followed by 48 h of incubation in rabbit anticalbindin 4°C (1:7,000, Swant) and 2% NHS. Subsequently, the sections were incubated overnight 4°C in biotinylated goat–antirabbit IgG (1 to 500; Vector) and ABC-HRP (Vector). At the end of the immunostaining, the sections were stained with 0.5% 3,3-diaminobenzidine tetrahydrochloride and 0.01% H_2O_2 for 15 min at room temperature. Ultimately, the sections were osmicated with 2% osmium in 8% glucose solution, dehydrated in dimethoxypropane, and stained en block with 3% uranyl acetate/70% ethanol for 60 min and embedded in Araldite (Durcupan, Fluka, Germany). Guided by findings in semithin sections, we made pyramids of the medial cerebellar nucleus, lateral cerebellar nucleus, interposed cerebellar nucleus, and superior vestibular nucleus. Ultrathin sections (70–90 nm) were cut using an Ultramicrotome (Leica, Germany), mounted on copper grids, and counterstained with uranyl acetate and lead citrate. Purkinje cell terminals were photographed and analyzed using an electron microscope (Philips, Eindhoven, The Netherlands). Electron micrographs were taken at magnifications ranging from ×1,500 to ×30,000 from single hole EM grids and analyzed with the use of commercially available software (SIS) to study diameters and surface areas of labeled terminals and their surrounding structures in the neuropil. The surface area measurements were deduced automatically by drawing the circumference of all profiles (IBAS systems). Terminals of the lateral cerebellar nucleus and interposed cerebellar nucleus were each quantified per 25,000 μm^2 in each animal by a researcher who was blind to the genotype of the mice. Since no significant differences were observed among the two cerebellar nuclei, the data were pooled. Statistics were done with the use of unpaired Student's *t* tests assuming equal variances. *p* values equal or smaller than 0.05 were considered significant.

Electrophysiology

Five *tg* mutants and five wild-type littermates of ~6–8 months were anesthetized with ketamine (50 mg/kg body weight) and xylazine (8 mg/kg body weight) and subjected to extracellular single unit recordings of neurons in the cerebellar nuclei. Borosilicate pipettes (OD 2 mm, ID 1.16 mm, 4–10 MΩ, ~1–2 μm tip diameter) filled with 2 M NaCl solution were positioned stereotactically using an electronic pipette holder (Luigs & Neumann, Ratingen, Germany). Signals were sampled at 10 KHz (Digidata 1322A, Axon Instr., Foster City, CA, USA), amplified, filtered, and stored for offline analysis (Multiclamp 700A, Axon Instr.). Purkinje cells in the cerebellar cortex were stimulated using custom-made urethane-insulated tungsten electrodes with two tips (separated ~25 μm). A single negative 100-μs pulse of 100–400 μA (Cornerstone BSI-950, Dagan, Minneapolis, MN, USA) was used to activate the surrounding cerebellar cortical tissue. Stimulus locations were never deeper than 0.5 mm and were positioned in Lobule VI or paramedian lobule. Neurons of the cerebellar nuclei were identified by recording their characteristic activities [26]. Once a responsive area within a cerebellar nucleus was found, multiple tracks were made to record both stimulus response activity and spontaneous activity. Evoked activity was recorded for at least 70 trials of 2 s each (at a frequency of 0.5 Hz) before or after which spontaneous activity was recorded for >2 min. Histological verification of the location of recordings was done by injection of 4% Alcian blue dye.

Analysis of Electrophysiological Data

Off-line analysis of neuronal firing rates was performed in Matlab (Mathworks Inc. Natick, MA, USA) as previously described by Goossens and colleagues [27]. Firing frequency, coefficient of variance (CV; standard deviation (SD) interspike interval/mean interspike interval), and peristimulus histograms of the extracellularly recorded neuronal activities in the cerebellar nuclei were constructed using custom made routines in Matlab (Mathworks). To identify statistically significant responses to electrical stimulation of the cerebellar cortex from peristimulus histograms, we constructed an analog representation of each spike train using Gaussian local rate coding [28]. The sum of these Gaussians represents the instantaneous firing frequency, which we normalized. Poststimulus excursions of the mean instantaneous frequency that exceeded three times the standard deviation were marked as statistically significant responses [26] and were used to specify the latency of the inhibition. We used a Gaussian width of 1 ms to determine the occurrence of the spike rate change, typically at <6 ms after the stimulus onset. Any spiking activity that occurred during the stimulus artifact was not included in the analysis. Statistical analysis was done using unpaired Student's *t* tests (two tailed) assuming equal variances. Differences were considered to be significant when the p value≤ 0.05. Data are presented as mean ± standard error of the mean.

Results

Light Microscopy

Immunohistochemical calbindin stainings labeled all parts of the Purkinje cells including their cell bodies, dendrites,

and axons in both wild types and *tg*s. Labeled Purkinje cell terminals were found throughout the medial cerebellar nuclei, lateral cerebellar nuclei, as well as the anterior and posterior interposed cerebellar nuclei (Fig. 1). In addition, many labeled terminals were observed in the medial vestibular nuclei and superior vestibular nuclei (Fig. 1a,b), while only few were observed in the nuclei prepositus hypoglossi (data not shown). In both wild types and *tg*s, labeled Purkinje cell terminals were mostly adjacent to cell bodies and proximal dendrites of their target neurons (see also [23]). No significant differences were observed among the densities of terminals in the lateral cerebellar nuclei and interposed cerebellar nuclei ($p=0.2$; $N=3$ for both wild type and *tg*) or between *tg*s and wild types (data of both cerebellar nuclei pooled; $p=0.7$; $N=3$).

Electron Microscopy

Five-Week-Old Animals The morphology and postsynaptic distribution of calbindin-labeled Purkinje cell terminals were initially analyzed in 5-week-old animals, as this is the age when ataxia is present for ~1–2 weeks [8]. Labeled Purkinje cell terminals as well as their nonmyelinated preterminal segments and myelinated axons could be readily identified in the various cerebellar nuclei and in the superior vestibular nucleus (Fig. 2). Purkinje cell terminals in wild types were densely packed with pleiomorphic vesicles and they established one or more symmetric synaptic contacts with the soma and/or a dendritic segment of their target neurons as described previously for rats ([23]; for criteria of synaptology, see also [29]; Fig. 2a). The vast majority of the Purkinje cell terminals included at least a few mitochondria, but some of them were filled with as many as ten mitochondria (see e.g., Fig. 2c). Purkinje cell terminals in *tg*s showed the same content of vesicles as well as the same type and distribution of synapses, but they were enlarged due to the presence of vacuoles (Fig. 2b,d).

Quantitative analyses of the Purkinje cell terminals ($N=3$ and $n=204$ for *tg*; $N=2$ and $n=158$ for wild type) of the 5-week-old animals at the ultrastructural level confirmed and extended the findings described above. First, we did not find any significant difference in the density of Purkinje cell terminals among wild types and *tg*s ($p=0.3$; Fig. 2e). Next, we showed that the terminals in *tg*s were indeed significantly enlarged ($p<0.01$) and that more terminals contained vacuoles ($p<0.05$; Fig. 2e,f) than in wild type. Moreover, of the terminals that did contain one or more vacuoles those in the *tg* contained a higher number of vacuoles ($p<0.05$). Similarly, the number of mitochondria per terminal tended to be increased in *tg*, which might

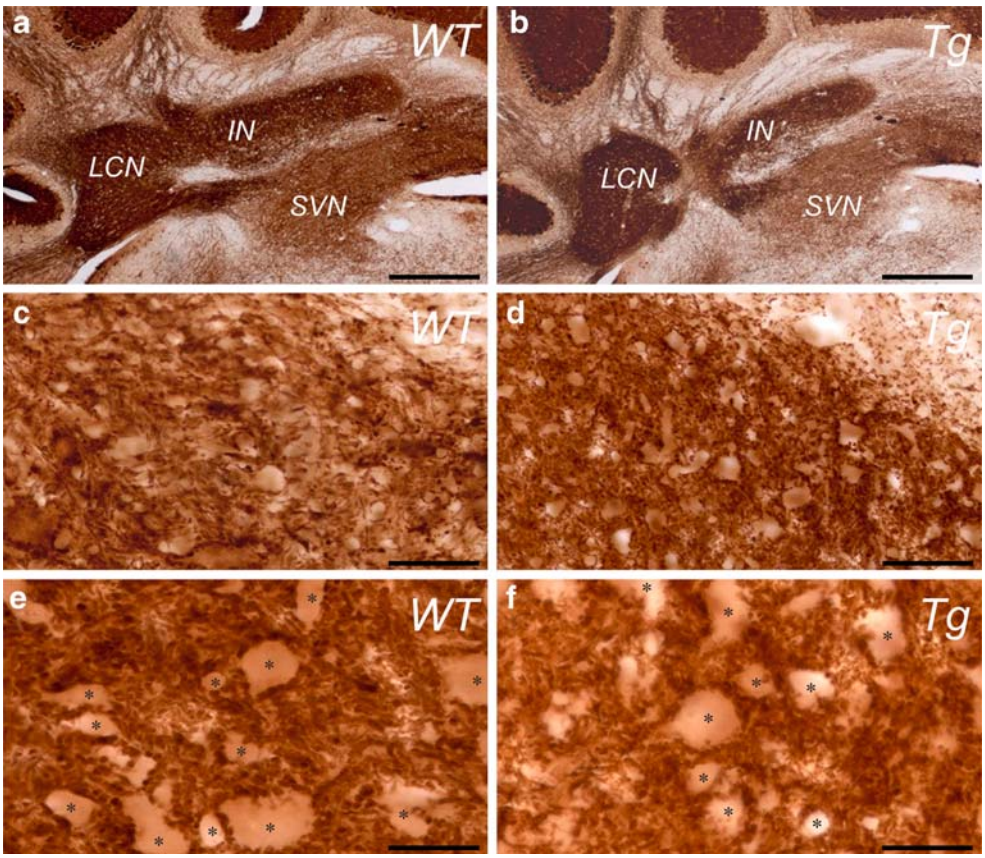

Fig. 1. Distribution of calbindin-labeled Purkinje cell terminals in the cerebellar and vestibular nuclei in wild types (*WT*) and tottering (*Tg*) at the light microscopic level. **a**–**b** Note the high densities of labeled terminals in the lateral cerebellar nucleus (*LCN*) and interposed nucleus (*IN*) and the intermediate density in the superior vestibular nucleus (*SVN*). **c**–**f** Higher magnifications show labeled Purkinje cell terminals opposed to the somata of neurons in the interposed cerebellar nuclei. *Asterisks* indicate somata of nuclear neurons. *Scale bars* indicate 450 μm in **a** and **b**, 75 μm in **c** and **d**, and 25 μm in **e** and **f**

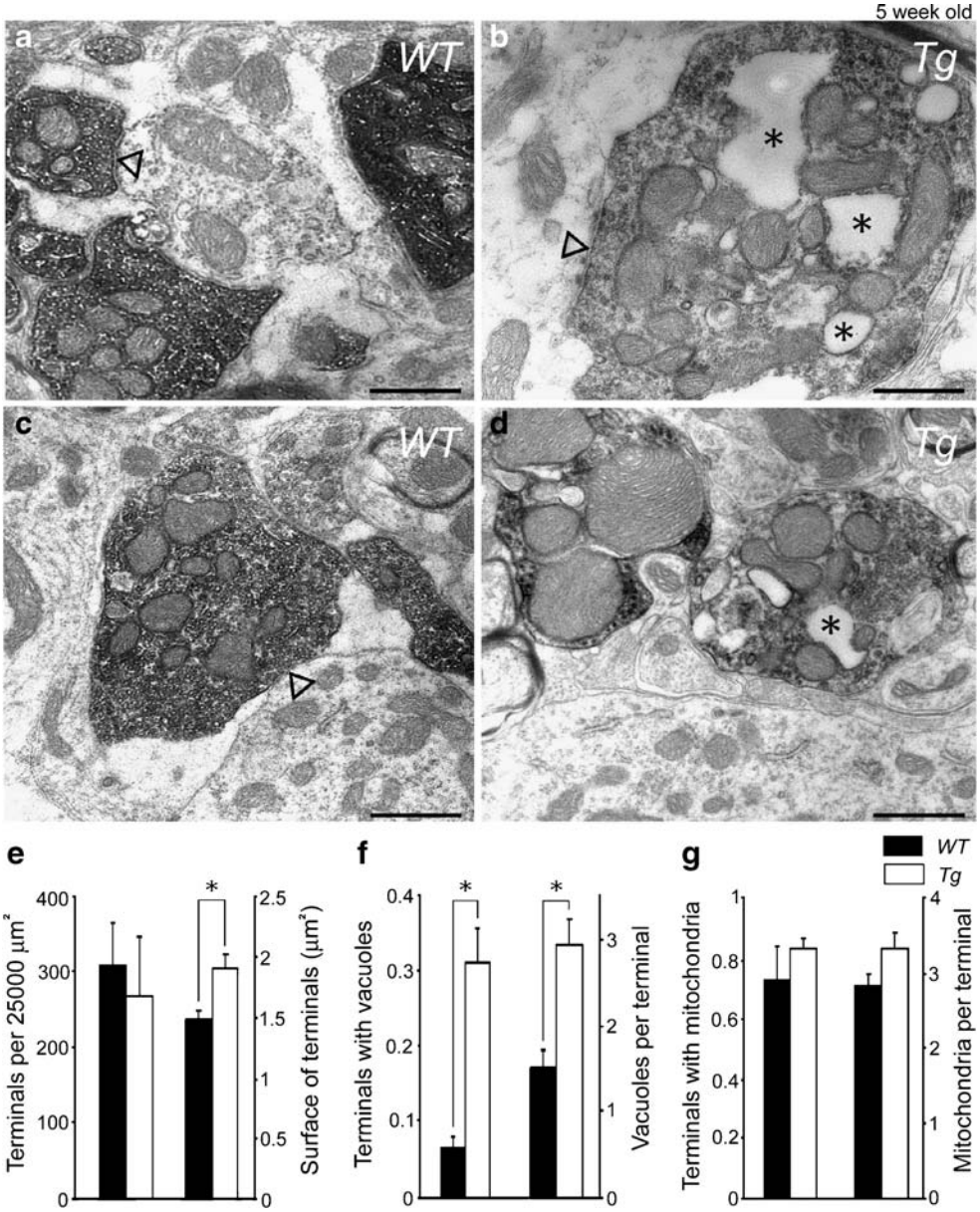

Fig. 2. Electron micrographs of calbindin-labeled Purkinje cell terminals taken from 5-week-old mice. **a**, **b** Purkinje cell terminals in the lateral cerebellar nucleus of wild types (*WT*) and tottering (*Tg*), respectively. **c**, **d** Purkinje cell terminals in the superior vestibular nucleus of WT and Tg, respectively. Note that the Purkinje cell terminals in Tg contain vacuoles (*asterisks*) and in some cases (*upper left corner* in **d**) swollen mitochondria. The terminals in **a**, **b**, and **c** establish symmetric synaptic contacts (*open triangles*). *Scale bar* in **a** indicates 550 nm, in **b** 350 nm, and in **c** and **d** 625 nm. **e**–**g** Histograms showing the morphological characteristics of Purkinje cell terminals in WT (*black*) and Tgs (*white*) in the cerebellar nuclei (*CN*). **e** Densities of terminals (*left*) and their surface areas (*right*). **f** Number of terminals that have vacuoles (*left*) and of those terminals, the average number of vacuoles per terminal (*right*). **g** Number of terminals with mitochondria (*left*) and of those terminals, the average number of mitochondria per terminal (*right*). *Asterisks* indicate significant differences

contribute to the enlargement of terminals (Fig. 2g). Still the number of terminals that contained mitochondria is not increased (p=0.9). To find out as to whether neurotransmission and/or compensatory synaptic mechanisms may take place in Purkinje cell terminals of 5-week-old *tg*s, we also quantified their number of synapses per terminal. We did not find any significant difference between wild types and mutants in this respect (p=0.3; Fig. 5).

Six-Month-Old Animals The analysis of the Purkinje cell terminals in 5-week-old *tg* animals showed that they were moderately but significantly enlarged and that they contained significantly more vacuoles, while their number of mitochondria tended to be slightly increased. To find out as to whether these pathologies persisted and/or deteriorated over time, we investigated the morphology of Purkinje cell terminals (N=3 and n=172 for *tg*; N=3 and n=211 for wild type) in the cerebellar nuclei of 6-month-old mice. Similar to the 5-week-old animals, the density of Purkinje cell terminals was not significantly reduced in the cerebellar nuclei of the 6-month-old *tg* mutants (p=0.4), while the average surface area of their terminals was significantly larger than that in their age-matched wild-type littermates (p<0.001; Fig. 3). This observation was corroborated by the findings that the average numbers of terminals that contained vacuoles and/or mitochondria were significantly larger in *tg* than those in wild-type littermates (p<0.001 and p<0.01, respectively). In addition, the number of vacuoles per terminal as well as the mitochondria per terminal was significantly (both p values<0.01) increased in these

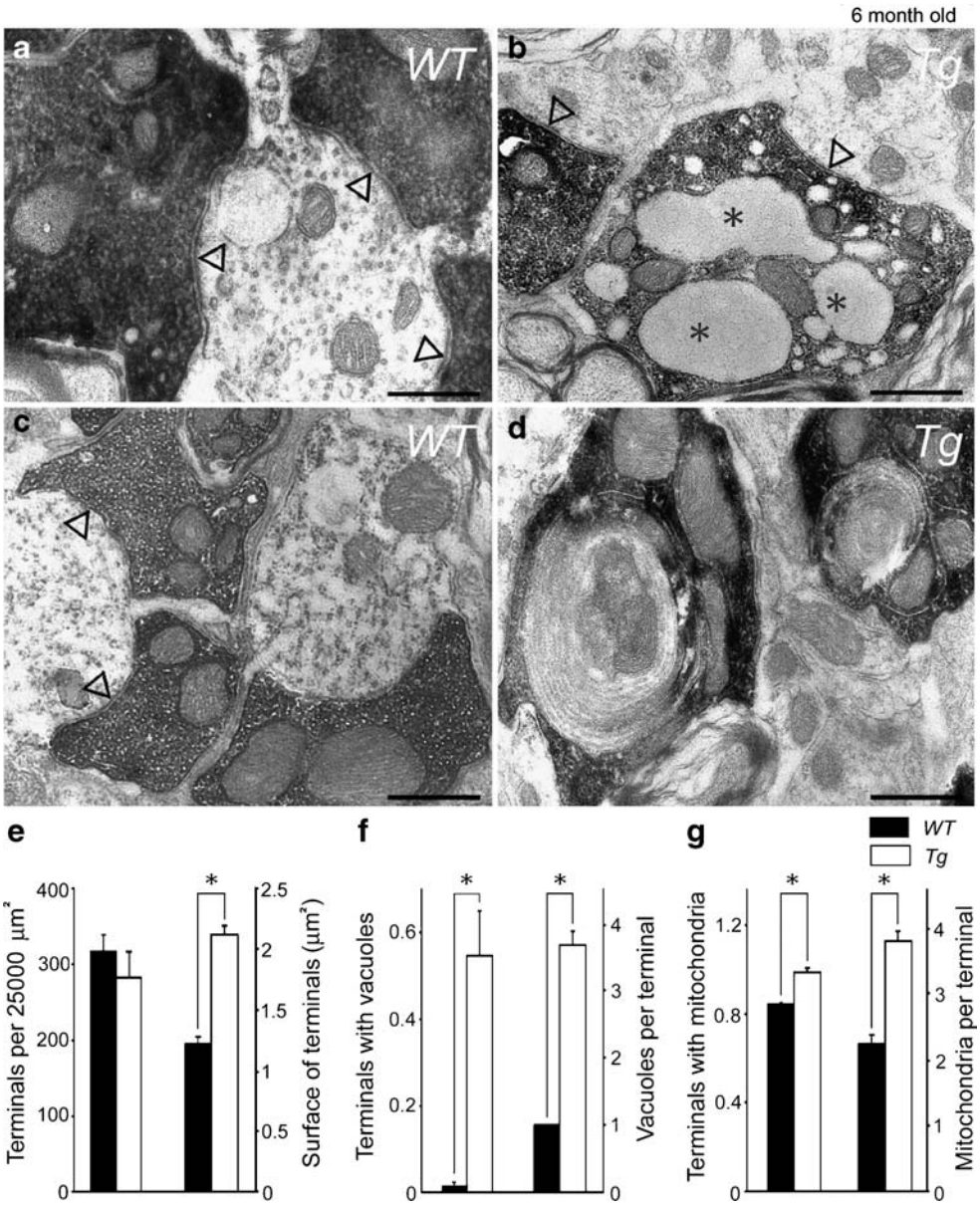

Fig. 3. Electron micrographs of calbindin-labeled Purkinje cell terminals taken from 6-month-old mice. **a**, **b** Purkinje cell terminals in the lateral cerebellar nucleus of wild types (*WT*) and tottering (*Tg*), respectively. **c**, **d** Purkinje cell terminals in the interposed cerebellar nucleus of wild type (**c**) and tottering (**d**). Note that the Purkinje cell terminals in tottering contain vacuoles (*asterisks* in **b**) and whorled bodies (membranous lamellar structures in **d**). The terminals in **a**, **b**, and **c** establish symmetric synaptic contacts (*open triangles*). *Scale bar* in **a** indicates 350 nm, in **b** and **c** 625 nm, and in **d** 550 nm. **e**–**g** Histograms showing the morphological characteristics of Purkinje cell terminals in the cerebellar nuclei of 6-month-old WTs (*black*) and Tgs (*white*). **e** Densities of terminals (*left*) and their surface areas (*right*). **f** Number of terminals that have vacuoles (*left*) and of those terminals, the average number of vacuoles per terminal (*right*). **g** Number of terminals with mitochondria (*left*) and of those terminals, the average number of mitochondria per terminal (*right*). *Asterisks* indicate significant differences

terminals. Interestingly, the morphology of the vacuoles got worse over time in that they showed more irregular shapes (compare Figs. 2 and 3) and that their number per terminal increased significantly ($p<0.05$) compared to 5-week-old *tg*s. Moreover, more *tg* terminals contained vacuoles at 6 months than at 5 weeks ($p<0.01$), whereas the wild-type terminals tended to show less vacuoles per terminal at 6 months then at 5 weeks of age ($p=0.16$). Similarly, the numbers of terminals that had mitochondria in the 6-month-old *tg*s were significantly higher than those in the 5-week-old *tg*s ($p<0.01$), but not in the wild types ($p=0.8$). The impact of the *tg* mutation on the Purkinje cell terminals in 6-month-old mice was further indicated by the presence of so-called whorled bodies (Fig. 3d). These large structures, which can also be observed in Purkinje cell terminals following olivary lesions and might be a result of increased production of smooth endoplasmic reticulum [22], were present in 7% of the terminals. Still, neurotransmission between the Purkinje cell terminals and their target neurons may still occur in these older *tg* mutants, because the number and structure of the synapses appeared intact as compared to wild types ($p=0.2$; Fig. 5). Thus, ultrastructural analyses of the cerebellar nuclei in the 6-month-old animals showed that the pathology of the Purkinje cell terminals in adult *tg* mutants progresses steadily, but they also suggest that synaptic neurotransmission is possible.

Two- to Three-Week-Old Animals If the morphological aberrations of the Purkinje cell terminals in *tg* contribute to their behavioral phenotype, one expects that these

abnormalities start to occur in the period when the ataxia start to occur, i.e., at the age of 3 to 4 weeks [8]. We therefore investigated whether the morphological abnormalities were already apparent at 2–3 weeks of age. Indeed, analysis of Purkinje cell terminals of these young animals did not show a significant difference among wild types (N=4; n=116) and *tg*s (N=4; n=118) for any of the morphological parameters described above (Fig. 4). Thus, the density and shape of the terminals as well as those of the mitochondria inside these terminals appeared normal, and there were no signs of pathology such as high numbers of vacuoles or whorled bodies or altered numbers of synapses (Fig. 5). The onset of the cytological abnormalities in the Purkinje cell terminals in *tg* must therefore occur between 3 and 5 weeks after birth.

Electrophysiology

The ultrastructural data described above showed that the numbers of synaptic contacts between Purkinje cells and their target neurons in the cerebellar nuclei are not affected in *tg* mutants (see also Fig. 5), while the content of the Purkinje cell terminals show signs of progressive pathology. These findings raise the questions as to whether synaptic neurotransmission is possible at the Purkinje cell terminals and, if so, whether the temporal pattern of the postsynaptic activity in the cerebellar nuclei neurons is normal. We therefore investigated the latency and duration of inhibition in the cerebellar nuclei neurons induced by activation of the Purkinje cells as well as the temporal pattern of spontaneous activities of the cerebellar nuclei neurons.

Purkinje cell stimulation in the cerebellar cortex of 6-month-old animals resulted in clear inhibition in the cerebellar nuclei neurons in both *tg* and wild type (Fig. 6). No differences were found among *tg* and wild-type mice in the threshold for eliciting an inhibitory response (p=0.4), and the latency and duration of these responses were also not significantly different. In responsive neurons, the firing was interrupted with a latency of 3.1±0.6 ms in *tg* and 4.2± 0.7 ms in wild type (n=7 for both genotypes; p=0.2; Fig. 6b), while the duration of the inhibition lasted 4.4± 0.7 ms in *tg* and 4.6±1.2 ms in wild type (n=7 for both genotypes; p=0.6). Apart from the initial inhibition, some

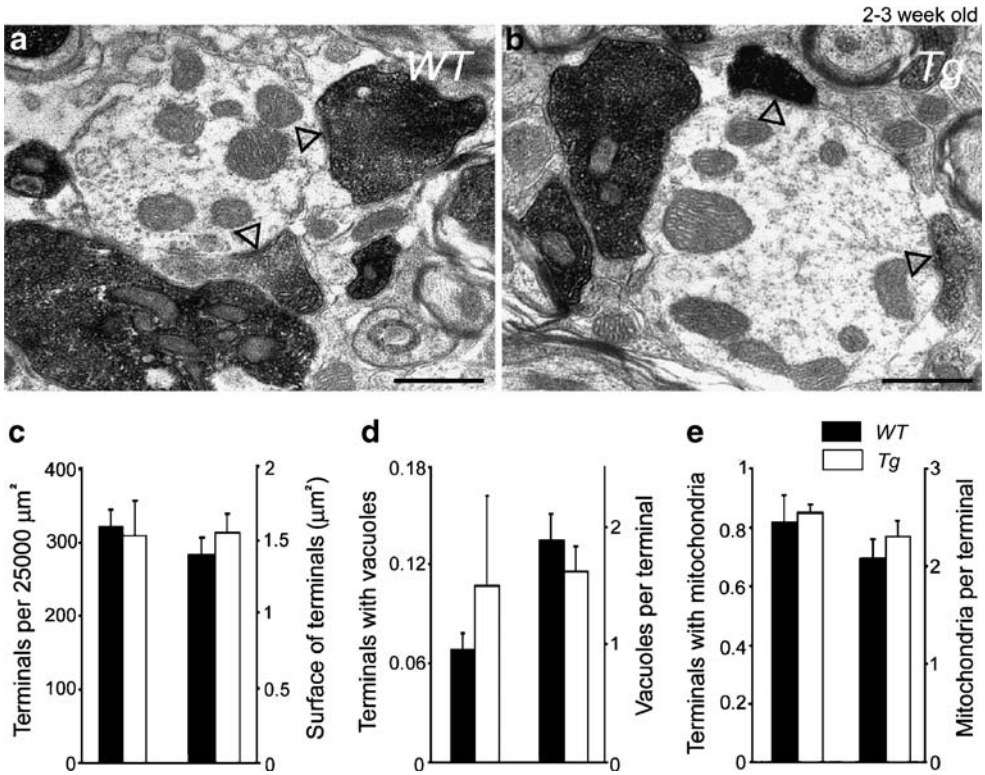

Fig. 4. Electron micrographs of calbindin-labeled Purkinje cell terminals taken from 2–3-week-old mice. **a**, **b** Purkinje cell terminals in the lateral cerebellar nucleus of wild types (*WT*) and tottering (*Tg*), respectively. Note that the Purkinje cell terminals in tottering do not contain pathological inclusions and that the terminals in **a** and **b** establish symmetric synaptic contacts (*open triangles*). *Scale bars* in **a** and **b** both indicate 625 nm. **c**–**e** Histograms showing the morphological characteristics of Purkinje cell terminals in the cerebellar nuclei of 2–3-week-old WT (*black*) and Tg (*white*). **c** Densities of terminals (*left*) and their surface areas (*right*), respectively. **d** Number of terminals that have vacuoles (*left*) and of those terminals, the average number of vacuoles per terminal (*right*). **e** Number of terminals with mitochondria (*left*) and of those terminals, the average number of mitochondria per terminal (*right*)

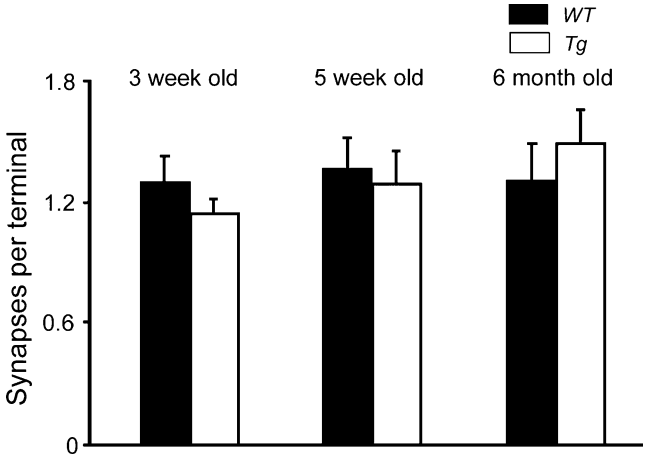

Fig. 5. Histograms showing the number of synapses per terminal for 3-week-old, 5-week-old, and 6-month-old wild-types (*WT*; *black*) and tottering mice (*Tg*; *white*). Note that no significant differences are found between the genotypes among any of the three different ages

cells responded with a consecutive increase in firing frequency (n=4 for both wild type and *tg*). The latency of this rebound excitation varied widely in both groups and was not significantly different (p=0.3) among the two genotypes (5.6±2.3 ms in *tg* and 7.7±2.4 ms in wild types). Thus, these data indicate that the Purkinje cell terminals are functionally intact when activated concertedly in an artificial fashion using electrophysiological stimulation.

The finding that neurotransmission at the synapses of the Purkinje cell terminals in the cerebellar nuclei of *tg* can occur following artificial electrical stimulation does not necessarily imply that this process operates normally under natural circumstances. We therefore also recorded spontaneous activities of the cerebellar nuclei neurons that receive Purkinje cell input (Fig. 7a). Long recordings of spontaneous activity showed that the average firing frequency of these neurons in the lateral and medial cerebellar nuclei of 6-month-old *tg* mice (64.7±3.6 Hz; N=5 and n=44) is significantly higher (p<0.01) than that of wild-type littermates (48.5±3.0 Hz; N=5 and n=70; Fig. 7b). In addition, the coefficient of variance of these spiking activities in *tg* (1.44±0.22) was significantly higher (p< 0.01) than that in wild types (0.99±0.1; Fig. 7c). These data are in line with the hypothesis that under physiological conditions, the inhibition imposed by the Purkinje cells onto the cerebellar nuclei neurons in *tg* is less effective and less consistent than that in wild types.

Discussion

The main finding of the present study is that Purkinje cell terminals in the cerebellar nuclei in *tg* show signs of structural damage such as an increase in size, swelling of mitochondria, presence of pathological vacuoles, and formation of large whorled bodies, while their synapses appear functionally intact. These morphological observations are corroborated by the finding that the activity patterns of their postsynaptic neurons in the cerebellar nuclei are faster and more irregular than those of their wild-type littermates. As will be discussed below, the morphological and physiological findings each have their own implications, but together they suggest that the pathology in Purkinje cell terminals in *tg* may contribute to a suboptimal neurotransmission in their cerebellar nuclei and thereby to their behavioural deficits.

The observation that the number of Purkinje cell terminals and synapses were not affected in *tg* agreed with the fact that we found normal latencies and duration values for inhibition in the cerebellar nuclei neurons following artificial stimulation of the Purkinje cell input. These findings are in line with the findings in *tg* that electrical stimulation of floccular Purkinje cells in their vestibulocerebellum can evoke short latency eye movements [9] and that cortical lesions in their anterior vermis can have a positive impact on the occurrence of intermittent myoclonus-like movements [30, 31]. Thus, neurotransmission appears possible at the synapses formed by the Purkinje cell terminals and their target neurons in the cerebellar and vestibular nuclei, but the question remains to what extent the pathology in the Purkinje cell terminals impairs signal coding.

The occurrences of swollen mitochondria and pathological vacuoles and to a lesser extent also those of the whorled bodies form the most prominent pathological changes that can be found in the Purkinje cell terminals of *tg* mice. The exact mechanisms by which these three phenomena can be explained remain to be shown, but several possibilities should be addressed. First, the Purkinje cell terminals in *tg* contain the mutated P/Q-type Ca^{2+}-channels and thereby they will most likely directly show altered dynamics and kinetics of their vesicle release, which in turn may influence the constitution of the organelles inside them [32–35]. Second, the increased irregularity of Purkinje cell firing in *tg* contributes to the occurrence of high frequency bursts of simple spikes [9]. Increased simple spike firing frequencies have been shown to affect the formation of vacuoles, mitochondria, smooth endoplasmatic reticulum, and cause the formation of whorled bodies, e.g., in response to lesions of the inferior olive [22, 36, 37]. Although the changes in simple spike firing in *tg* are not as profound as seen in wild-type animals after lesioning the inferior olive, the effects in *tg* are chronic and could therefore amount to a similar effect on Purkinje cell terminals. For example, Rossi and colleagues showed that the formation of vacuoles, mitochondria, smooth endoplasmatic reticulum, and whorled bodies were all affected in a

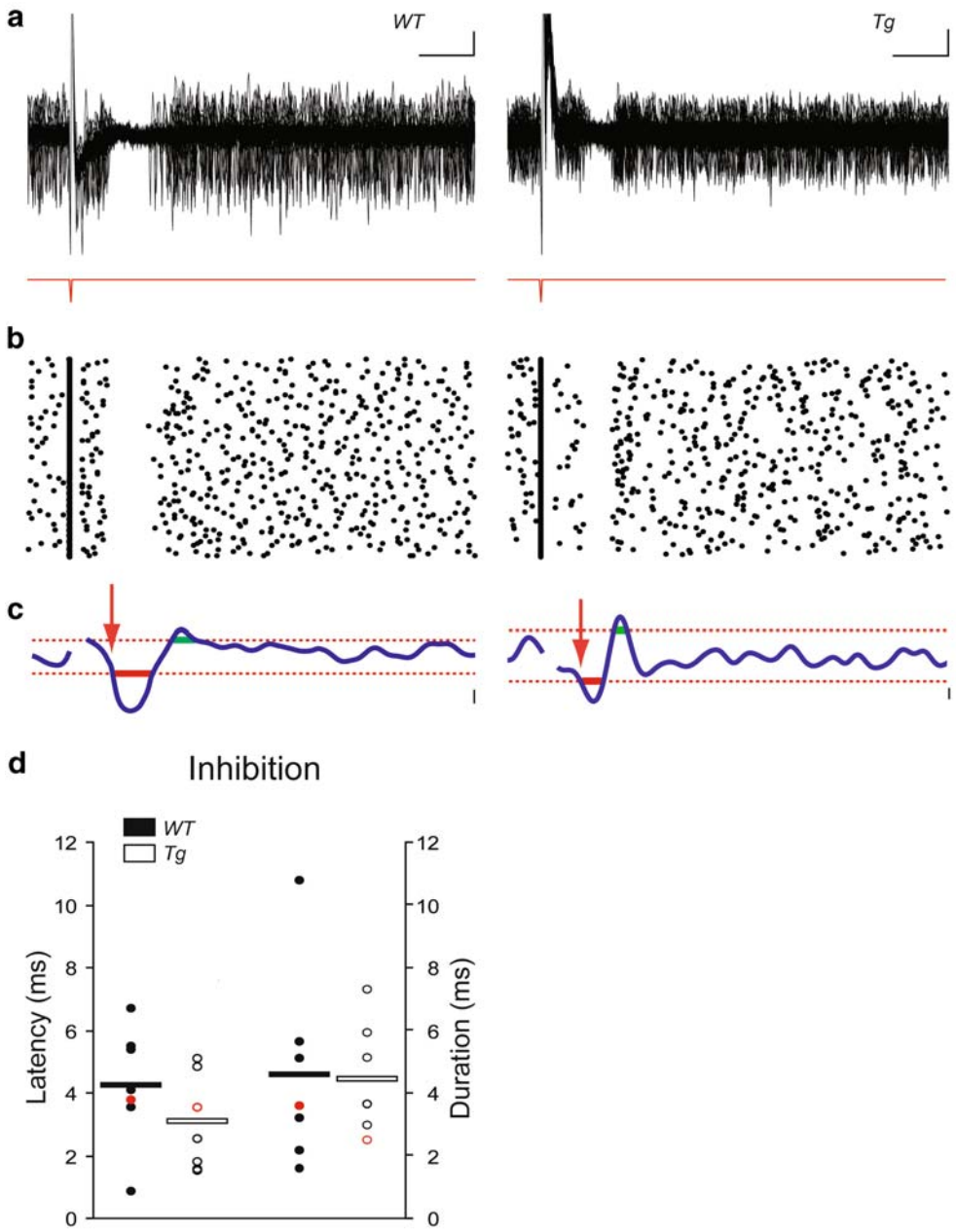

Fig. 6. Cerebellar nuclei neurons responding to stimulation of Purkinje cells in the cerebellar cortex of 6-month-old wild-type and tottering mice. **a** Overlay of 100 traces of a single unit recording from an interposed nucleus neuron of a wild-type (*WT*; *left panel*) and tottering (*Tg*; *right panel*) mouse. *Scale bars* indicate 500 μV (*vertical*) and 5 ms (*horizontal*) in the *left panel* and 200 μV (*vertical*) and 5 ms (*horizontal*) in the *right panel*. Dip in lower trace indicates stimulus pulse of 100 μs. **b** Accompanying scatter plot of single unit activity showing the same period of inhibition as in **a**. **c** Gaussian fit with a 1-ms time constant. *Solid blue line* indicates the mean Gaussian fit and the *dotted horizontal lines* indicate ±3 SD used to calculate the latency (see "Materials and Methods" section for details). Note that both these wild-type and tottering cells responded with a significant inhibition (*solid red line*) followed by a significant excitation (*solid green line*; see text for details). *Vertical scale bars* indicate 0.3 and 0.2 normalized frequency in the *left and right panel*, respectively. **d** Average latency (*left*) and duration of the inhibition (*right*) following stimulation of the cerebellar cortex. *Dots* indicate values of individual recordings and *horizontal bars* indicate the average values per genotype. *Red dots* (wild type) and *circles* (*Tg*) indicate the latency and duration of the inhibition for the examples used in **a**

dynamic fashion in particular time frames after lesioning the olive. Presumably, the changes in smooth endoplasmic reticulum that were observed by Rossi and colleagues, but not by us, were directly related to those of the whorled bodies [38, 39], which were in fact also more substantial in their study than in the current one [22]. Therefore, the chronic occurrence of high frequency bursts in Purkinje cell activity in *tg* may trigger multiple intracellular mechanisms,

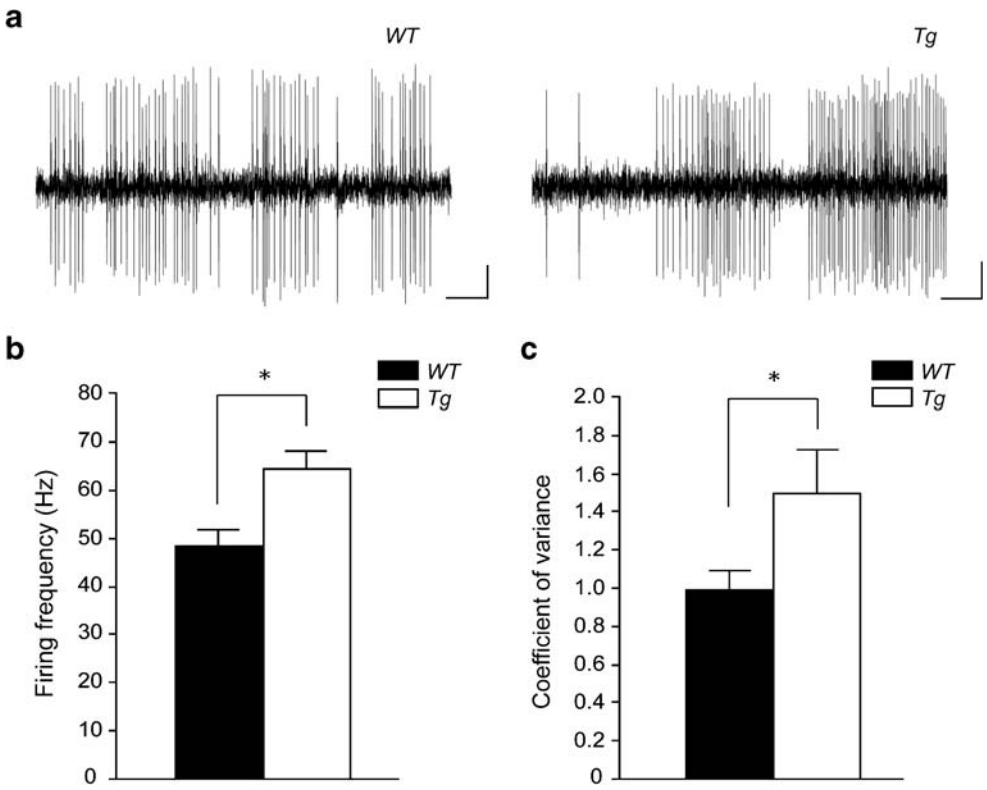

Fig. 7. Activity patterns of cerebellar nuclei neurons of 6-month-old wild-type and tottering mice. **a** Typical examples of extracellular recordings of cerebellar nuclei neurons from the lateral dentate nucleus of a wild-type (*WT*, *left panel*) and tottering (*Tg*, *right panel*) mouse. *Scale bars* indicate 200 μV (*vertical line*) and 100 ms (*horizontal line*). **b** Average firing frequencies found in wild type and tottering; note the increased level in tottering. **c** Average coefficients of variance found in wild type and tottering; note the increased level in tottering

which in turn could lead to the increase of the number and volume of mitochondria as well as the formation of vacuoles and whorled bodies within the same terminals.

The findings described and discussed above raise the question to what extent the pathological aberrations in the Purkinje cell terminals in *tg* interact with those in their dendrites and cell bodies and to what extent they both contribute to the cerebellar movement disorders [9, 16, 17]. The possibility that the pathological process at the terminals interacts with that at the cell body and dendritic arbor and that they both contribute to the behavioral deficits is supported by the observation that the period in which the morphological aberrations in the terminals start to occur, i.e., between the third and fifth postnatal week, coincides with the period in which the dendrites show their first abnormalities and in which the first signs of ataxia start to occur [8, 17]. Moreover, it should be noted that abnormalities occurring in the axons themselves may also interact with those in the dendrites and terminals. In older *tg*s (>6 months), the axons also show signs of swelling with accumulations of cytoplasmic organelles, irregularly arranged microtubules, and inclusions of a lysosomal origin [17, 18], raising the possibility that propagation of action potentials down the Purkinje cell axons can also be affected in these *tg* mice. Such a deficit may be especially detrimental, because during burst activity, the simple spike frequency in *tg* mice can even exceed the maximum frequency that can be transmitted down the Purkinje cell axon in a healthy rodent [9, 40, 41]. Thus, since the swelling and abnormalities that occur in the axons and terminals may further reduce this maximum frequency in *tg*, the synaptic efficacy of the high frequency simple spike bursts at their cerebellar nuclei neurons will be even lower. This reduced efficacy may add to the more direct cell physiological deficits caused by the mutated P/Q-type voltage-gated calcium channels in Purkinje cell terminals that will affect their machinery of neurotransmitter release, as has also been shown for other cerebellar GABAergic inhibitory synapses [42–44]. Taken together, our previous and present results provide ample evidence that the information relayed by the Purkinje cells in *tg* mice is scrambled due to the altered synaptic input and decreased calcium influx in their dendrites and somata, and we propose that the ultrastructural aberrations in the axons and terminals further scramble their pathological spiking pattern. Thus, we conclude that the ultrastructural aberrations in the axonal terminals of the Purkinje cells in *tg* described in the current study are likely to contribute to their cerebellar movement disorders.

The question remains to what extent the neurons in the cerebellar nuclei show intrinsic abnormalities in *tg* mice. Our current results show that in vivo these neurons fire action potentials more irregular and faster and one may argue that this manifestation of aberrant information processing could be due to the fact that P/Q-type calcium channels are also expressed in cerebellar nuclei neurons

themselves [11, 45, 46]. However, recent evidence shows that the impact of P/Q-type calcium channels on the intrinsic excitability of cerebellar nuclei neurons is minimal [47], which stands in sharp contrast to their impact on the excitability of Purkinje cells [48]. Still, the cerebellar nuclei are formed by various types of excitatory and inhibitory neurons, which all have different electrophysiological characteristics [47, 49, 50]. Thus, in order to further clarify the origin of cerebellar movement disorders in calcium mutants such as the *tg* we do not only need to address the transmission of the Purkinje cell to cerebellar nuclei neuron synapse but also the intrinsic excitability of each type of neuron in the cerebellar nuclei.

Conclusions

In conjunction, we conclude that the abnormalities at the Purkinje cell terminals in *tg* are likely to interact with those at their dendrites and cell bodies and that they probably all contribute to an impaired output of the cerebellar nuclei neurons and thereby to the ataxia.

Acknowledgments The authors thank Ing. E. Haasdijk for her excellent assistance. Furthermore, we like to thank Ing. J. van den Burg and M. Rutteman for technical assistance and Dr. T. Ruigrok for helpful comments and discussions. Research was supported by Neuro-Bsik, ZonMw, EUR-Fellowship, NWO-ALW, EEC-SENSOPAC, and Prinses Beatrix Fonds.

References

1. Noebels JL, Sidman RL (1979) Inherited epilepsy: spike-wave and focal motor seizures in the mutant mouse tottering. Science 204:1334–1336
2. Heller AH, Dichter MA, Sidman RL (1983) Anticonvulsant sensitivity of absence seizures in the tottering mutant mouse. Epilepsia 24:25–34
3. Kaplan BJ, Seyfried TN, Glaser GH (1974) Spontaneous polyspike discharges in an epileptic mutant mouse (tottering). Exp Neurol 66:577–586
4. Fureman BE, Jinnah HA, Hess EJ (2002) Triggers of paroxysmal dyskinesia in the calcium channel mouse mutant tottering. Pharmacol Biochem Behav 73:631–637
5. Campbell DB, Hess EJ (1998) Cerebellar circuitry is activated during convulsive episodes in the tottering (tg/tg) mutant mouse. Neuroscience 85:773–783
6. Campbell DB, Hess EJ (1999) L-Type calcium channels contribute to the tottering mouse dystonic episodes. Mol Pharmacol 55:23–31
7. Shirley TL, Rao LM, Hess EJ, Jinnah HA (2008) Paroxymal dyskinesias in mice. Mov Disord 23:259–64
8. Green MC, Sidman RL (1962) Tottering—a neuromusclar mutation in the mouse. And its linkage with oligosyndacylism. J Hered 53:233–237
9. Hoebeek FE, Stahl JS, van Alphen AM, Schonewille M, Luo C, Rutteman M et al (2005) Increased noise level of Purkinje cell activities minimizes impact of their modulation during sensorimotor control. Neuron 45:953–965
10. Stahl JS, James RA, Oommen BS, Hoebeek FE, De Zeeuw CI (2006) Eye movements of the murine P/Q calcium channel mutant tottering, and the impact of aging. J Neurophys 95:1588–1607
11. Fletcher CF, Lutz CM, O'Sullivan TN, Shaughnessy JD Jr., Hawkes R, Frankel WN et al (1996) Absence epilepsy in tottering mutant mice is associated with calcium channel defects. Cell 87:607–617
12. Pinto A, Gillard S, Moss F, Whyte K, Brust P, Williams M et al (1998) Human autoantibodies specific for the alpha1A calcium channel subunit reduce both P-type and Q-type calcium currents in cerebellar neurons. Proc Natl Acad Sci U S A 95:8328–8333
13. Llinás RR, Sugimori M, Cherksey B (1989) Voltage-dependent calcium conductances in mammalian neurons. The P channel. Ann NY Acad Sci 560:103–111
14. Mintz IM, Venema VJ, Swiderek KM, Lee TD, Bean BP, Adams ME (1992) P-type calcium channels blocked by the spider toxin omega-Aga-IVA. Nature 366:156–158
15. Wakamori M, Yamazaki K, Matsunodaira H, Teramoto T, Tanaka I, Niidome T et al (1998) Single tottering mutations responsible for the neuropathic phenotype of the P-type calcium channel. J Biol Chem 273:34857–34867
16. Matsushita K, Wakamori M, Rhyu IJ, Arii T, Oda S, Mori Y et al (2002) Bidirectional alterations in cerebellar synaptic transmission of tottering and rolling Ca2+ channel mutant mice. J Neurosci 22:4388–4398
17. Rhyu IJ, Abbott LC, Walker DB, Sotelo C (1999) An ultrastructural study of granule cell/Purkinje cell synapses in tottering (tg/tg), leaner (tg(la)/tg(la)) and compound heterozygous tottering/leaner (tg/tg(la)) mice. Neuroscience 90:717–728
18. Meier H, MacPike AD (1971) Three syndromes produced by two mutant genes in the mouse. Clinical, pathological, and ultrastructural bases of tottering, leaner, and heterozygous mice. J Hered 62:297–302
19. Isaacs KR, Abbott LC (1992) Development of the paramedian lobule of the cerebellum in wild-type and tottering mice. Dev Neurosci 14:386–393
20. Hillman D, Chen S, Aung TT, Cherksey B, Sugimori M, Llinás RR (1991) Localization of P-type calcium channels in the central nervous system. Proc Natl Acad Sci U S A 88:7076–7080
21. Catterall WA (1999) Interactions of presynaptic Ca2+ channels and snare proteins in neurotransmitter release. Ann NY Acad Sci 868:144–159
22. Rossi F, Cantino D, Strata P (1987) Morphology of Purkinje cell axon terminals in intracerebellar nuclei following inferior olive lesion. Neuroscience 22:99–112
23. De Zeeuw CI, Berrebi AS (1995) Postsynaptic targets of Purkinje cell terminals in the cerebellar and vestibular nuclei of the rat. Eur J Neurosci 7:2322–2333
24. Teune TM, van der Burg J, De Zeeuw CI, Voogd J, Ruigrok TJ (1998) Single Purkinje cell can innervate multiple classes of projection neurons in the cerebellar nuclei of the rat: a light microscopic and ultrastructural triple-tracer study in the rat. J Comp Neurol 392:164–178
25. Baurle J, Grusser-Cornehls U (1994) Calbindin D-28k in the lateral vestibular nucleus of mutant mice as a tool to reveal Purkinje cell plasticity. Neurosci Lett 167:85–88
26. Rowland NC, Jaeger D (2005) Coding of tactile response properties in the rat deep cerebellar nuclei. J Neurophysiol 94:1236–1251

27. Goossens HH, Hoebeek FE, Van Alphen AM, Van Der Steen J, Stahl JS, De Zeeuw CI et al (2004) Simple spike and complex spike activity of floccular Purkinje cells during the optokinetic reflex in mice lacking cerebellar long-term depression. Eur J Neurosci 19:687–697, Erratum in: Eur J Neurosci. 2004;19:1673
28. Paulin MG (1996) System identification of spiking sensory neurons using realistically constrained nonlinear time series models. In: Gath I, Inbar G (eds) Advances in processing and pattern analysis of biological signals. Plenum, New York, pp 183–194
29. De Zeeuw CI, Holstege JC, Ruigrok TJ, Voogd J (1989) Ultrastructural study of the GABAergic, cerebellar, and mesodiencephalic innervation of the cat medial accessory olive: anterograde tracing combined with immunocytochemistry. J Comp Neurol 284:12–35
30. Campbell DB, North JB, Hess EJ (1999) Tottering mouse motor dysfunction is abolished on the Purkinje cell degeneration (pcd) mutant background. Exp Neurol 160:268–278
31. Abbott LC, Bump M, Brandl A, De Laune S (2000) Investigation of the role of the cerebellum in the myoclonic-like movement disorder exhibited by tottering mice. Mov Disord 15(Suppl 1):53–59
32. Heuser J, Katz B, Miledi R (1971) Structural and functional changes of frog neuromuscular junctions in high calcium solutions. Proc R Soc Lond B Biol Sci 178:407–415
33. Hirokawa N, Heuser JE (1981) Structural evidence that botulinum toxin blocks neuromuscular transmission by impairing the calcium influx that normally accompanies nerve depolarization. J Cell Biol 88:160–171
34. Sutton KG, McRory JE, Guthrie H, Murphy TH, Snutch TP (1999) P/Q-type calcium channels mediate the activity-dependent feedback of syntaxin-1A. Nature 401(6755):800–804, Oct 21
35. Garcia AG, Garcia-De-Diego AM, Gandia L, Borges R, Garcia-Sancho J (2006) Calcium signaling and exocytosis in adrenal chromaffin cells. Physiol Rev 86:1093–131
36. Desclin JC, Colin F (1980) The olivocerebellar system. II. Some ultrastructural correlates of inferior olive destruction in the rat. Brain Res 187:29–46
37. Strata P, Montarolo PG (1982) Functional aspects of the inferior olive. Arch Ital Biol 120:321–329
38. Ikemoto T, Yorifuji H, Satoh T, Vizi ES (2003) Reversibility of cisternal stack formation during hypoxic hypoxia and subsequent reoxygenation in cerebellar Purkinje cells. Neurochem Res 28:1535–1542
39. Takei K, Mignery GA, Mugnaini E, Südhof TC, De Camilli P (1994) Inositol 1,4,5-trisphosphate receptor causes formation of ER cisternal stacks in transfected fibroblasts and in cerebellar Purkinje cells. Neuron 12:327–342
40. Khaliq ZM, Raman IM (2005) Axonal propagation of simple and complex spikes in cerebellar Purkinje neurons. J Neurosci 12:454–463
41. Monsivais P, Clark BA, Roth A, Hausser M (2005) Determinants of action potential propagation in cerebellar Purkinje cell axons. J Neurosci 25:464–472
42. Caillard O, Moreno H, Schwaller B, Llano I, Celio MR, Marty A (2000) Role of the calcium-binding protein parvalbumin in short-term synaptic plasticity. Proc Natl Acad Sci U S A 97:13372–13377
43. Stephens GJ, Morris NP, Fyffe RE, Robertson B (2001) The Cav2.1/alpha1A (P/Q-type) voltage-dependent calcium channel mediates inhibitory neurotransmission onto mouse cerebellar Purkinje cells. Eur J Neurosci 13:1902–1912
44. Satake S, Saitow F, Rusakov D, Konishi S (2004) AMPA receptor-mediated presynaptic inhibition at cerebellar GABAergic synapses: a characterization of molecular mechanisms. Eur J Neurosci 19:2464–2474
45. Chung YH, Shin C, Park KH, Cha CI (2000) Immunohistochemical study on the distribution of neuronal voltage-gated calcium channels in the rat cerebellum. Brain Res 865:278–282
46. Sawada K, Sakata-Haga H, Ando M, Takeda N, Fukui Y (2001) An increased expression of Ca(2+) channel alpha(1A) subunit immunoreactivity in deep cerebellar neurons of rolling mouse Nagoya. Neurosci Lett 316:87–90
47. Alvina K, Khodakhah K (2008) Selective regulation of spontaneous activity of neurons of the deep cerebellar nuclei by N-type calcium channels in juvenile rats. J Physiol 586(10):2523–2538
48. Womack M, Khodakhah K (2003) Active contribution of dendrites to the tonic and trimodal patterns of activity in cerebellar Purkinje neurons. J Neurosci 15:10603–10612
49. Uusisaari M, Obata K, Knopfel T (2007) Morphological and electrophysiological properties of GABAergic and non-GABAergic cells in the deep cerebellar nuclei. J Neurophysiol 97:901–911
50. Uusisaari M, Knopfel T (2008) GABAergic synaptic communication in the GABAergic and non-GABAergic cells in the deep cerebellar nuclei. Neuroscience 156:537–549